Study on Half Quantum Vortices in Superconductors

Guru Kalyan Jayasingh

170260025

ENGINEERING PHYSICS, SENIOR YEAR

Supervised by

Alexander Zyuzin

Researcher, Department of Applied Physics,

Aalto University, Finland

Sumiran Pujari

Assistant Professor, Dept. of Physics, IIT Bombay

Contents

Chapter 1

Introduction

In recent years, an increasing amount of studies have been made on the phenomena of unconventional superconductivity. In addition to usual $U(1)$ symmetry, these states can break a host of other symmetries (crystal rotational symmetry, time reversal etc.) and can lead to novel thermodynamic and transport properties which aren't seen in usual s-wave pairing.

Currently, the phenomenon of superconductivity in $M_x Bi_2 Se_3$ has been of some interest (particularly $Cu_x Bi_2 Se_3$ which is a doped topological insulator).[2] proposed that the inter-orbital odd parity pairing symmetry in a strongly spin orbit coupled normal state might be an explanation for the same. As analysed in [2], this can happen only in the presence of a two component order parameter. However, as commented in [3], the current understanding still remains unconclusive as to the nature of the pairing. It is in this regard that the current thesis aims to study one aspect of this problem, namely, the phenomenon of half quantum vortices present possible in this material. The organisation of this thesis is as follows: In chapter 1 half quantum vortices (HQV) are analysed using the framework of ginzburg landau theory. A concrete realisation of this model is highlighted in a microscopic example carried in chapter 2. This then helps to provide for a calculation of spin polarization around vortex states, which is computed for the case of a overlapping HQV pair. Finally, the thesis concludes with some comments on the experimental significance of the spin polarization.

Chapter 2

Half Quantum Vortices in a nematic Superconductor

2.1   Ginzburg-Landau analysis

We start by considering the free energy functional for two order parameters. The construction is based on symmetry arguments done in [5]. This will again be derived from a microscopic theory in the coming chapter. For the time being we take the form of the functional defined in the paper directly and try to motivate the physics associated with different terms appearing in the GL functional.

 We assume the system to be uniform along the c direction of the lattice, thus making the model effectively two dimensional.Nematic superconductivity is modeled by two component order parameters (defined as η_x, η_y) which arrive from the gap matrix $\Delta_{\alpha\beta} = [(\vec{d}\cdot\vec{\sigma})i\sigma_y]_{\alpha\beta}$ with $\vec{d}(\vec{k}) = \hat{z}(\eta_x sin(k_x a) + \eta_y sin(k_y a))$ where a is the lattice constant in the xy plane. The order parameter transforms as a 2D vector under spatial rotation. However, one can identify (due to the two dimensional nature) $\vec{\eta}$ with $-\vec{\eta}$, hence it is best to think of this vector as the nematic director. This also makes it possible to have a unique vector perpendicular to $\vec{\eta}$, hence we can expect a dual theory in terms of this $\vec{\eta}_\perp$. Following [3], the functional is written as in η_x, η_y basis as

$$F = \alpha(\eta_i^*\eta_i) + \frac{\beta_1}{2}[(\eta_i^*\eta_i)^2 + \beta|\eta_i\eta_i|^2] + \frac{(\nabla\times\vec{A})^2}{8\pi} + K_1(p_i\eta_j)^*(p_i\eta_j)$$
$$+K_2(p_i\eta_i)^*(p_j\eta_j) + K_3(p_i\eta_j)^*(p_j\eta_i) \qquad (2.1)$$

 where i = (x,y), $p_i = -\partial_i + A_i$ (where the units as chosen such that $\bar{h} = -\dfrac{e^*}{c} = 1$). The form of the above functional becomes more transparent if we define the same in chiral basis $\eta_\pm = \eta_x \pm i\eta_y$. Define $p_\pm = p_x \pm ip_y$ to get

$$F = \frac{\alpha}{2}(|\eta_+|^2 + |\eta_-|^2) + \frac{\beta_1}{8}(|\eta_+|^4 + |\eta_-|^4) + \frac{\beta_1 \delta\beta}{2}(|\eta_+|^2|\eta_-|^2) + \frac{K_{13}}{4}(|p_+\eta_+|^2 + |p_-\eta_-|^2)$$

$$+ \frac{K_{12}}{4}(|p_+\eta_-|^2 + |p_-\eta_+|^2) + \frac{K_{23}}{4}[(p_+\eta_-)^*(p_-\eta_+) + (p_-\eta_+)^*(p_+\eta_-)] \tag{2.2}$$

where $K_{ij} = K_i + K_j$ and $\delta\beta = 1/2 + \beta$. We can see that the first two terms resemble the usual GL functional, while the third term couples both order parameters at the quartic level. If we set $K_2 = K_3$, then we see that the first two gradient terms also resemble the usual s-wave case, effectively making this two copies of the usual s-wave. The final term describes the mixed gradient coupling between both the order parameters, thus enabling the possiblity of modulating the spatial profile in a coupled way in presence of a magnetic field.

[1] analyzed this model and positivity of the free energy led to the following constraints on the various coefficients:

$$\beta_1 > 0 \quad \beta > -1 \quad K_1 > 0 \quad 1 > C > \frac{-1}{3} \tag{2.3}$$

where $C = \frac{K_2 + K_3}{2K_1}$.

2.2 Uniform Solutions (without $\vec{A}$)

In order to solve for the OPs in this case, gradient terms don't contribute. Taking only the homogenous parts, we have the free energy functional

$$F = \alpha(\eta_i^* \eta_i) + \frac{\beta_1}{2}[(\eta_i^* \eta_i)^2 + \beta|\eta_i \eta_i|^2] \tag{2.4}$$

To solve this system, we set the OP as $\vec{\eta} = \eta_\infty e^{i\chi(x)} \begin{bmatrix} cos(\theta(x)) \\ e^{i\psi(x)} sin(\theta(x)) \end{bmatrix}$ where $\theta(x)$ is some global phase, $\psi(x)$ is a phase difference between order parameters and η_∞ is the value of magnitude of the OP. Clearly for the uniform case, we have θ, α, ψ independent of $\vec{x}$. This yields two solutions:

- Case 1: $\beta > 0$ We have the form of solution as $\vec{\eta} = \eta_\infty e^{i\chi(x)} \begin{bmatrix} 1 \\ \pm i \end{bmatrix}$ with $\eta_\infty^2 = \frac{-\alpha}{\beta_1}$. This solution corresponds to Chiral Phase.

- Case 2: $-1 < \beta < 0$ We have the form of the solution as $\vec{\eta} = \eta_\infty e^{i\chi} \begin{bmatrix} cos(\theta) \\ sin(\theta) \end{bmatrix}$. This solution corresponds to nematic phase.

While the chiral preserve the rotational symmetry (but breaks Time reversal), the nematic phase breaks spontaneous rotational symmetry. We focus on the nematic phase as it's a proposed theoretical candidate for superconductivity in $M_x Bi_2 Se_3$ (for e.g. $Cu_x Bi_2 Se_3$).

2.3 Half Quantum Vortices: Structure

Consider the nematic solution in absence of $\vec{A} = 0$ - It consists of two variables, orientation variable α and angular phase variable θ. Topologically speaking, a phase vortex of the usual s-wave nature involves winding of the phase variable by 2π, however, from the looks of the solution, we can imagine that one can equivalently construct a single valued OP by winding each of θ and α by π. This would imply that the vortex encompasses half quantum of vortex. Quantitatively

$$\chi = n_p \frac{\phi}{2}, \theta = \theta_\infty + \frac{n_0 \phi}{2} \tag{2.5}$$

where θ_∞ is the orientation at $\phi = 0$ (ϕ being the azimuthal angle). We define (n_p, n_0) as the topological charges, associated respectively with phase and orientation winding. This is the reason why this structure is called half quantum vortex, the phase variable winds only by during a full rotation.
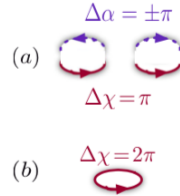

Figure 2.1: HQV vs PV pair winding depiction: While a PV winds by 2π in it's phase, HQV winds π in each of it's dof

Once we ship to the chiral basis, we find that the structure of vortices become

$$(\eta_+, \eta_-) = \eta_\infty \left(exp(i \frac{n_p + n_o}{2} \phi + i \frac{\theta_\infty}{2}), \ exp(i \frac{n_p - n_0}{2} \phi - i \frac{\theta_\infty}{2}) \right) \propto (e^{i \pm \phi}, 1) \ or \ (1, e^{\pm i \phi}) \tag{2.6}$$

Hence every half quantum vortex (HQV) corresponds to one full vortex of η_+(or η_-) with in a constant non-zero background of η_-. In this convention phase vortex takes topological charge (± 2,0). This representation also allows combining two HQVs with the rule

$$(\pm 1, 1) + (\pm 1, -1) = (\pm 2, 0) \tag{2.7}$$

This can be easily seen by considering each of the above as a single vortex in chiral basis that add up.

In a usual super-conductor phase gradient is screened at long distances due to the meissner effect, and the gradient energy is localized around the face vertex and remains finite. However, since the orientation gradient remains unscreened, the energy cost associated with it diverges system size. However, for a pair of half quantum vortices, orientation gradient energy becomes finite and hence is a stable configuration. Therefore half quantum vortices must always come in pairs with opposite orientation topological charge (n_0).

Numerically, the presence of this HQV structure was done in [6], where the simulation observed stable configuration of a HQV pair and two pairs of HQV.
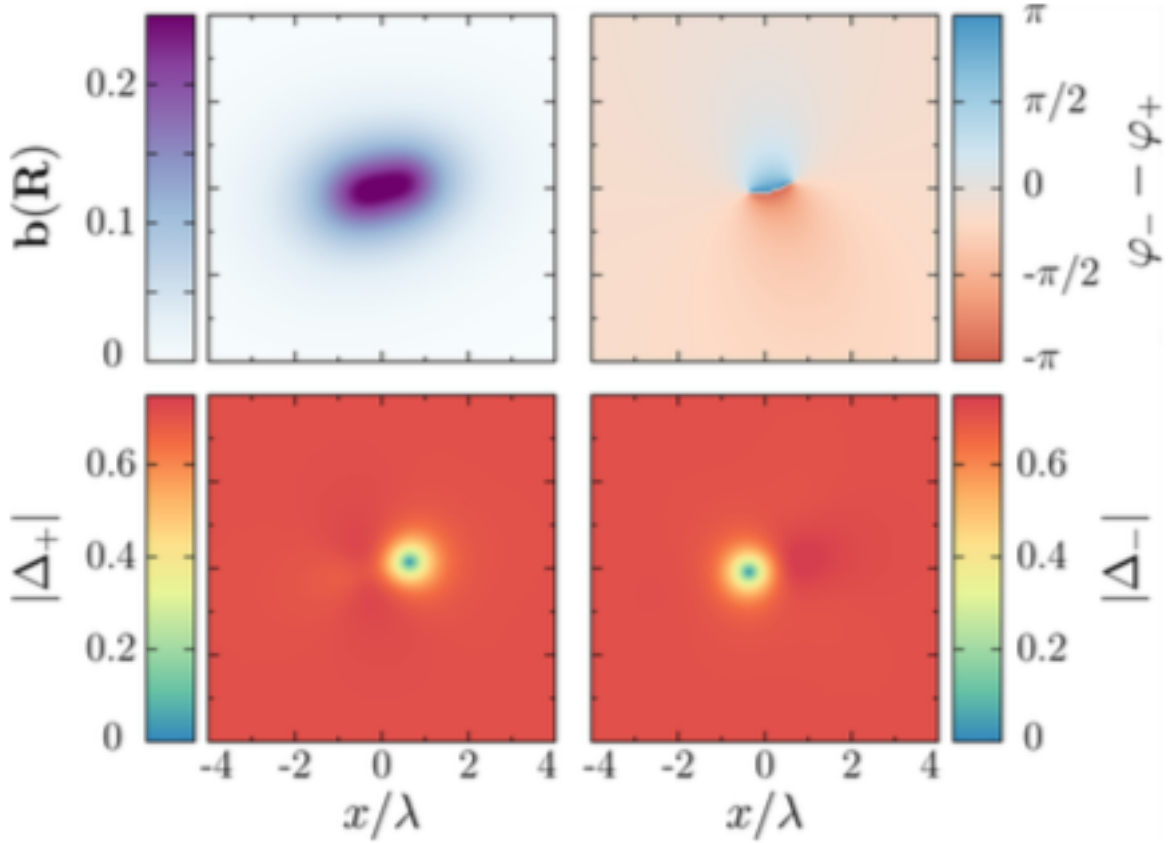

Figure 2.2: Figure depicts $\vec{B}, \Delta_{\pm}$ for a HQV pair. On the first line, the first panel shows the distribution of the magnetic field, while the second displays the relative phase between the two components of the order parameter. The second line shows the densities of the two components of the order parameter. Clearly, the cores in both components do not superimpose. Since cores do not overlap, the rel- ative phase has $\pm 2\pi$ winding around each core. Taken from [6]

This then raises the interesting question which goes as follows: does a pair of HQV's

essentially merge into a single phase vortex or does it remain as a tightly bound pair at a finite separation?

2.4 Stability analysis for HQV pair: London Limit

Following [3] we consider the extreme London limit where $|\vec{\eta}|$ is is uniform everywhere except at the core of the vortices. For very large separation, gauge field $\vec{A}$ gets screened out and hence energy in the gauge sector separates for both. However, $\nabla\theta$ gradient energy is still finite and nonzero in the region in between the vortices, but does not diverge with system size. This interaction is a decreasing function of d, the inter-vortex separation. Hence at these separations, the vortices attaract each other.

Now when the separation is $d < \lambda$, $\vec{A}$ is still uniform while phase gradients are in place. In the London limit, the free energy is given by

$$F = Z[|\nabla\theta|^2 + |\nabla\chi|^2] + g[(\hat{u} \times \nabla\theta)^2 + (\hat{u} \cdot \nabla\chi)^2 - (\hat{u} \cdot \nabla\theta)^2 - (\hat{u} \times \nabla\chi)^2] \qquad (2.8)$$

where $\hat{u} = (cos(\theta), sin(\theta))$ is the orientation unit vector, $Z = K_1|\alpha|(1 + C)/(\beta_1(1 + \beta_1))$, and $g = C/(1 + C)$. We see that on setting $K_2 = K_3 = 0$ (i.e. setting the mixed gradient terms in GL eqn(2) as zero, which amounts to setting $g \to 0$), we get a simple form of the F. The duality in this theory amounts to the transformation $\theta \to \theta + \frac{\pi}{2}, Z \to Z, \ g \to -g$.

Since $g = \dfrac{C}{1 + C}$, we can treat it perturbatively for $-1 < C < \frac{1}{3}$, as it's maximum value is 0.5 in that range. To gain some physical intuition about the g prefixed terms, let's set $\nabla\chi \to 0$ (because ultimately it'll get screened due to Gauge field). Now the remaining term $g((\hat{u} \times \nabla\theta)^2 - (\hat{u} \cdot \nabla\theta)^2)$, which can be understood as (for $g > 0$) rewarding alignment of $\hat{u}$ with $\nabla\theta$ while penalising mis-alignment or orthogonal alignment of $\hat{u}$. wrt $\nabla\theta$. Similarly for $g < 0$.

For a pair of vortices. The net energy of the pair can be broken down into

$$F_{pair} = 2F_{core} + F_{dipole} + F_{log} \qquad (2.9)$$

where F_{core} it's just the free energy of a single vortex (due to supercurrents and gauge sector), F_{log} is the logarithmic interaction energy (scaling roughly as $log(d)$, for the d being the separation between the 2 vortices) and F_{dipole} is a dipole potential depends on the relative alignment of the pair to the background $\vec{\eta}$ at infinity.

We now consider the solution for a single isolated of quantum vortex. The GL eqn corresponding to eqn (10) is now solved to yield (for a general winding of n_p and n_0, not necessarily integers)

$$\theta = \theta_\infty + \frac{n_0 \phi}{2} + \frac{g}{4} \frac{n_0^2 + n_p^2 - 4n_0}{(2 - n_0)^2} sin[(2 - n_0)\phi - 2\theta_\infty] \tag{2.10}$$

$$\chi = \frac{n_p \phi}{2} + \frac{g}{2} \frac{n_p}{(2 - n_0)} sin[(2 - n_0)\phi - 2\theta_\infty] \tag{2.11}$$

We see that there are residual parts other than the usual winding, however, they don't change the topological charge associated with a vortex. However, this eqn doesn't apply for $n_0 = 2$.

Once we have this, we plug it back into eqn(10) to get the core energy as

$$F_{core} = Z\pi ln(\Lambda/\xi)\left(1 - \frac{g^2}{2} + O(g^4)\right) \tag{2.12}$$

We see that the free energy is even in g due to the duality $g \to -g$. The length scales Λ and ξ curb the formally divergent expansion and impose short and long distance cutoffs. Λ governs both the screening length of the gauge sector and orientation gradient cost which is divergent which system size. However, given a pair of vortices, the orientation gradient energy is finite and limited by the intervortex separation. For the dipole as shown in the figure below
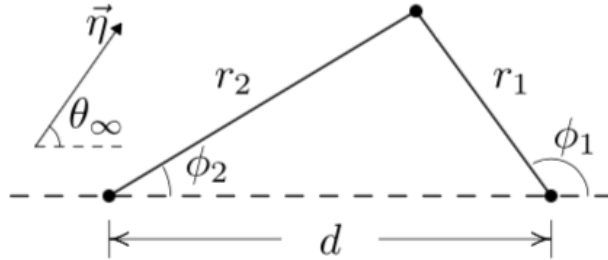

Figure 2.3: Taken from [3]

with a (1,-1) and (1,1) vortex on the left and the right respectively. The dipole energy is then given by utilising the zeroth order solution (in g) to the HQV yielding

$$\chi = \frac{\phi_1 + \phi_2}{2} + \dots \tag{2.13}$$

$$\theta = \theta_\infty + \frac{\phi_1 - \phi_2}{2} + \dots \tag{2.14}$$

This yields the dipole energy as

$$F_{dipole} = Z\pi cos(2\theta_\infty)(-g\pi + O(g^3)) \tag{2.15}$$

Since under duality implies $\theta_\infty \to \theta_\infty + \frac{\pi}{2}$, we need to have an odd series in g on the

RHS to make the F even. The dipole potential aligns $\vec{\eta}$ parallel to (or $\perp$ to) θ_∞ if C is positive (or subsequently negative).

To find F_{log}, we demand that the expression for $2F_{core}$ match with F_{PV} when the separation is limiting to zero. And equating the logarithmic parts on both sides, we get

$$F_{log} = Z\pi ln(\Lambda/d)\Big(- \frac{g^2}{4} + O(g^4)\Big)$$

This makes sure that when $d \to \xi$, we recover the PV energy of $F = Z\pi ln(\Lambda/\xi)\Big(2 - \frac{5}{4}g^2 + O(g^4)\Big)$. This shows that as we reduce d, F_{log} reduces and hence we see an attractive behaviour.

2.5 When cores overlap significantly

We would now like to investigate if the cores collapse into a single PV or due to repulsion, they form a bound state at finite separation. Now one has to do a complete GL analysis, by taking into account the non-linear structure of the core.

To estimate the free energy cost, we shift to the chrial basis where a HQV is interpreted as one vortex of $\eta_\pm$. We place them side by side with cylindrical shape. The form of the OP is chosen to be

$$(\eta_+, \eta_-) = \eta_\infty\big(e^{i(\phi_1+\theta_\infty)}f(r_1),\ f(r_2)e^{i(\phi_2-\theta_\infty)} \big) \tag{2.16}$$

with $\eta_\infty = \sqrt{-\alpha/[2\beta_!(1 + \beta)]}$, $\phi_{1,2}$ same as shown in the diagrams. We choose $f(r) = \Theta(\frac{r}{\xi} - 1) + \frac{r}{\xi}\Theta(1 - \frac{r}{\xi})$ as the amplitude variation of the OPs. Also assume that core overlap is significant i.e. $d \ll \xi$.

As shown in the paper by Yip etal in [3] , the terms that decide collapse or separation are terms in F that couple both η_+ and η_-. It is shown that the terms eventually lead to

$$F_{int} = K_1 C \frac{\eta_\infty^2}{2} cos(2\theta_\infty)I_{23} + \beta_1\delta\beta\eta_\infty^4 I_\beta$$

where I_{23}, I_β are two integrals are decreasing functions of d (i.e. as you increase d, they tend to decrease). Now depending upon the values of the parameters $\delta\beta, C$, HQV can separate or collapse. Also, depending on the sign of C, the pair dipole has an alignment which is same as what we have just below eqn (15) (there seems to be a sign error in the paper at this point, but nonetheless the phase diagram has been drawn correctly).
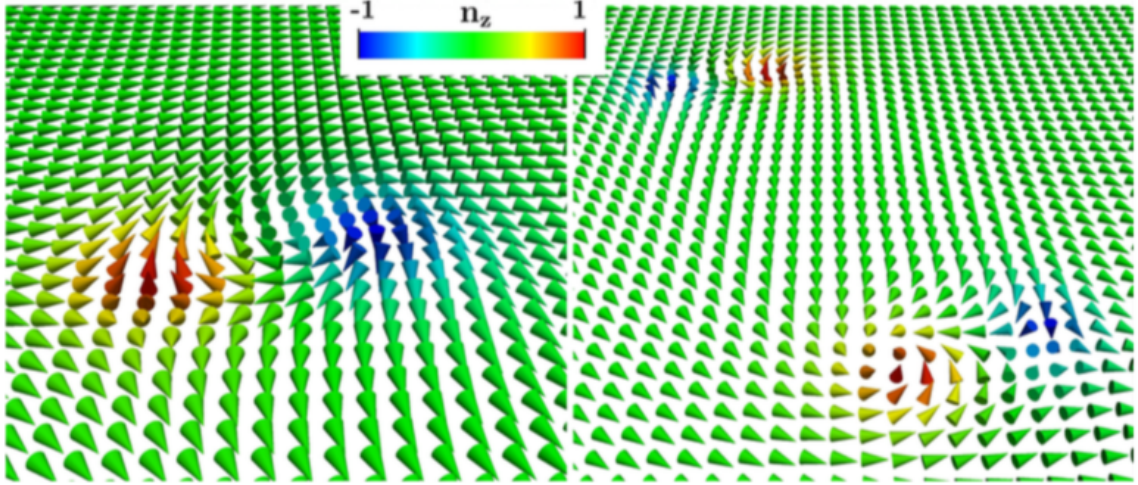
Figure 2.4: Texture of the unit vector n defined as the projection of the superconducting degrees of freedom onto the spin-1/2 Pauli matrices.The left panel shows a single-quanta solution, while the right panel correspond to the bound state of two HQV pair. Taken from [6]

2.6   Summary

We conclude this chapter with a summary of what was explored: We started with the expression of GL functional for a 2order parameter theory and explored the uniform solutions of the same. It was found that the theory can settle in two states: Namely nematic and chiral states, breaking rotational and time reversal symmetries respectively. Since the nematic phase is a candidate for superconductivity in $M_xBi_2Se_3$, an exploration of it's low field excitations in presence of a gauge field was explored (since the material is strongly type 2). This resulted in the interesting case of Half quantum vortex, which allows for both orientation and phase to wind, presenting itself as an extension to the conventional idea of a topological defect as PV. Further, by examining the energetics of an isolated HQV, it's unstability was shown and finally the interesting case of collapse. vs bound pair formation for a pair of HQV separated by a large distance initially was analysed. This study would prove fruitful in the next chapter where an exact microscopic derivation of the GL functional would be done and this idea of HQV would once again be analysed.

Chapter 3

Model Calculations

In this chapter, a model of 3D topological insulator is considered, with particular emphasis on Bi_2Se_3. The treatment followed here is a brief review of [6], which acts as a concrete realisation of the model constructed in the previous chapter.

3.1 Bi_2Se_3

Bi_2Se_3, the mother compound of the doped Bi2Se3 superconductors, has been extensively studied as a prototypical topological insulator. This compound has a rhombohedral (or trigonal) crystal structure.
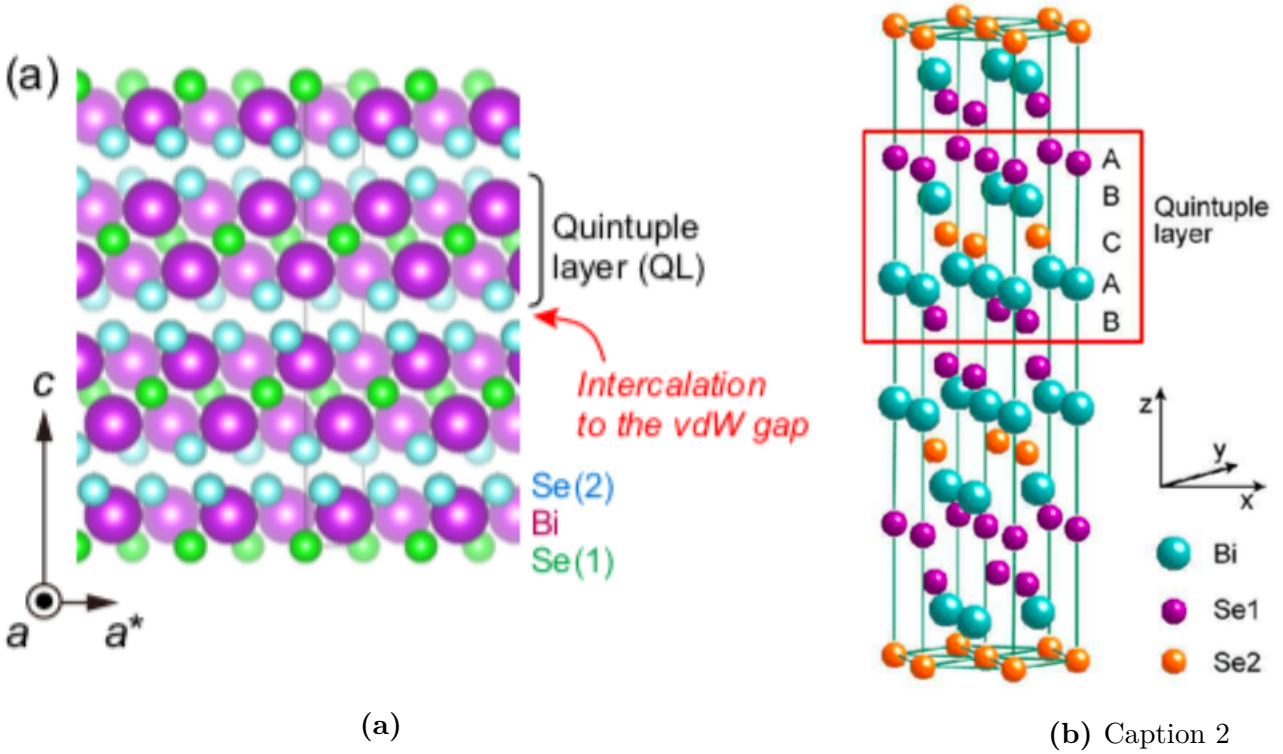

(a)

(b) Caption 2

Figure 3.1: Schematic description of the crystal structure of the mother compound Bi2Se3

The crystal structure consists of Se-Bi-Se-Bi-Se layers, called the quintuple layer (QL). Between the QLs, there is a van-der Waals (vdW) gap, through which metallic ions penetrate the sample during the synthesis process.

In 2010, the pioneering work by Hor et al. revealed that $Cu_xBi_2Se_3$ exhibits superconductivity below the critical temperature Tc of around 3 K. It was found that the electronic band structure of CuxBi2Se3 is essentially the same as that of Bi_2Se_3 and that the surface state originating from the topological-insulator nature of Bi_2Se_3 still exists even after the Cu doping.

Just after the discovery of superconductivity in $Cu_xBi_2Se_3$ [45], Fu et al.[2] performed theoretical analysis on possible SC states realized in this compound.The result is quite surprising since odd-parity topological superconductivity was predicted even with a simple pairing interaction. Previously, it had been believed that an unconventional pairing glue such as ferromagnetic spin fluctuation is required to realize bulk odd-parity superconductivity. Very naively, the odd-parity superconductivity in this model originates from strong orbital mixing on the Fermi surface; when a Cooper pair is formed among electrons in different orbitals, odd-parity superconductivity is rather easily realized.

3.2   Model Hamiltonian

The hamiltonian of the system is given by $H = \int d^3\vec{r}\, \Psi(\vec{r})^\dagger H(\vec{r})\Psi(\vec{r})$

$$H(\vec{r}) = v\tau_z\Big[\vec{\sigma} \times (-i\vec{\nabla} - \frac{e}{c}\vec{A})\Big]\cdot\hat{z} + v_z\tau_y\Big(-i\nabla_z - \frac{eA_z}{c}\Big) + m\tau_x \tag{3.1}$$

where in which v and v_z are the in-plane and out of plane components of the Fermi velocity, $\vec{A}$ is the gauge field, m is the hopping between different orbitals of Bi_2Se_3, $\vec{\sigma}$ are the Pauli matrices corresponding to spin operators and $\vec{\tau}$ are the pauli matrices corresponding to pseudospin degrees of freedom (1,2), $e < 0$ is electronic charge. The Electron operator is given by $\Psi(\vec{r}) = (\Psi_{\uparrow,1}(\vec{r}),\ \Psi_{\downarrow,1}(\vec{r}),\ \Psi_{\uparrow,2}(\vec{r}),\ \Psi_{\downarrow,2}(\vec{r}))$. Any zeeman contribution has been neglected for the time being. The dispersion in absence of magnetic field is given by $E_\pm = \sqrt{v^2p_\perp^2 + v_z^2p_z^2 + m^2}$, which is gapped at $\vec{p} = 0$ with magnitude 2m.

3.3   BCS pairing in this model

Pairing via BCS interaction in s-wave channel can happen in multiple ways (singlet intraorbital pairing, singlet interorbital pairing, triplet interorbital pairing), so there are multiple choices to make for gap parameter. The general pairing hamiltonian can be written as

$$H_{int} = -\sum_\tau \int d^3\vec{r}\, \Psi_{\downarrow\tau}^\dagger\Psi_{\uparrow\tau}^\dagger U_\tau \Psi_{\uparrow\tau}\Psi_{\downarrow\tau} - \lambda\sum_{\sigma,\sigma'}\int d^3\vec{r}\, \Psi_{\sigma 1}^\dagger\Psi_{\sigma' 2}^\dagger\Psi_{\sigma' 2}\Psi_{\sigma 1} \tag{3.2}$$

12

Defining $\Delta_\tau(\vec{r}) = U_\tau\langle\Psi_{\uparrow\tau}(\vec{r})\Psi_{\downarrow\tau}(\vec{r})\rangle$ and $\Delta_{\sigma\sigma'}(\vec{r}) = \lambda\langle\Psi_{\sigma 2}(\vec{r})\Psi_{\sigma'1}(\vec{r})\rangle$. Correspondingly, one defines $\Delta_\tau^\dagger = U_\tau\langle\Psi_{\downarrow\tau}^\dagger(\vec{r})\Psi_{\uparrow\tau}^\dagger(\vec{r})\rangle$ and $\Delta_{\sigma\sigma'}^\dagger = \lambda\langle\Psi_{\sigma 1}^\dagger(\vec{r})\Psi_{\sigma'2}^\dagger(\vec{r})\rangle$. Here Δ_τ characterises interorbital spin singlet pairing, while $\Delta_{\sigma\sigma'}$ characterizes both interorbital spin singlet and triplet pairings. Also see that we've taken zero harmonics of the electron-phonon interaction since they give higher transition temperature.

Now the complete BCS hamiltonian in expanded form looks like

$$
H_{bcs} = \int d^3\vec{r}\Psi^\dagger(\vec{r})\Big[v\tau_z\big[\vec{\sigma}\times(-i\vec{\nabla}-\frac{e}{c}\vec{A})\big]+v_z\tau_y\Big(-i\nabla_z-\frac{e\vec{A}_z}{c}\Big)+m\tau_x-\mu\Big]\Psi(\vec{r})
$$
$$
-\sum_\tau\int d^3\vec{r}\Big[\Delta_\tau^\dagger(\vec{r})\Psi_{\uparrow\tau}(\vec{r})\Psi_{\downarrow\tau}(\vec{r})+\Delta_\tau(\vec{r})\Psi_{\downarrow\tau}^\dagger(\vec{r})\Psi_{\uparrow\tau}^\dagger(\vec{r})-\frac{|\Delta_\tau(\vec{r})|^2}{U\tau}\Big]
$$
$$
-\sum_{\sigma\sigma'}\int d^3\vec{r}\Big[\Delta_{\sigma\sigma'}^\dagger(\vec{r})\Psi_{\sigma'2}(\vec{r})\Psi_{\sigma 1}(\vec{r})+\Delta_{\sigma'\sigma}(\vec{r})\Psi_{\sigma 1}^\dagger(\vec{r})\Psi_{\sigma'2}^\dagger(\vec{r})-\frac{|\Delta_{\sigma\sigma'}(\vec{r})|^2}{\lambda}\Big] \quad (3.3)
$$

Then we pick the nambu basis as $\Phi^\dagger = \big(\Psi^\dagger, \Psi^T(\vec{r})(-i\sigma_y)\big)$, where the second component is understood as : $\{\Psi^T(\vec{r})(-i\sigma_y)\}^\dagger = i\sigma_y(\Psi_{\uparrow,1}^\dagger,\Psi_{\downarrow,1}^\dagger,\Psi_{\uparrow,2}^\dagger,\Psi_{\downarrow,2}^\dagger)^T$ and the σ_y acts on the spin indices of each individual operator only. In this basis, the hamiltonian is given by

$$
H_{bcs} = \int d^3\vec{r}\Phi^\dagger(\vec{r})H_{BCS}(\vec{r})(\vec{r})\Phi(\vec{r})+\int d^3\vec{r}\Big[\sum\frac{|\Delta_\tau(\vec{r})|^2}{U_\tau}+\frac{|\Delta_{\sigma\sigma'}(\vec{r})|^2}{\lambda}\Big] \quad (3.4)
$$

where the matrix $H_{BCS}(\vec{r}) = \begin{bmatrix} H(\vec{r}) & \Delta(\vec{r}) \\ \Delta^\dagger(\vec{r}) & -\sigma_y H^*(\vec{r})\sigma_y \end{bmatrix}$, with each block being a 4×4 matrix. The gap matrix is denoted by

$$
\Delta(\vec{r}) = \frac{(\Delta_1(\vec{r}+\Delta_2(\vec{r}))}{2}+\frac{\Delta_1(\vec{r})-\Delta_2(\vec{r})}{2}\tau_z+\begin{bmatrix}\Delta_{\uparrow\downarrow} & \Delta_{\downarrow\downarrow} \\ -\Delta_{\uparrow\uparrow} & -\Delta_{\downarrow\uparrow}\end{bmatrix}\tau_+-\begin{bmatrix}\Delta_{\downarrow\uparrow} & \Delta_{\downarrow\downarrow} \\ -\Delta_{\uparrow\uparrow} & -\Delta_{\uparrow\downarrow}\end{bmatrix}\tau_- \quad (3.5)
$$

where $\tau_\pm = \frac{\tau_x\pm i\tau_y}{2}$.

Neglecting spin singlet inter-orbital pairing can be written as $\Delta(\vec{r}) = \frac{\Delta_1(\vec{r})+\Delta_2(\vec{r})}{2}+\frac{\Delta_1(\vec{r})-\Delta_2(\vec{r})}{2}\tau_z+\vec{\sigma}\cdot\vec{\Delta}(\vec{r})\tau_y$, where $\vec{\Delta}(\vec{r}) = (\Delta_x(\vec{r}),\Delta_y(\vec{r}),\Delta_z(\vec{r}))$ with $\Delta_x(\vec{r}) = -i\frac{\Delta_{\uparrow\uparrow}-\Delta_{\downarrow\downarrow}}{2}$, $\Delta_y(\vec{r}) = -\frac{1}{2}(\Delta_{\uparrow\uparrow}+\Delta_{\downarrow\downarrow})$ and $\Delta_z(\vec{r}) = \frac{1}{2}(\Delta_{\uparrow\downarrow}+\Delta_{\downarrow\uparrow})$. In this we've assumed inter-orbital spin singlet pairing to be 0 i.e. $\Delta_{\uparrow\downarrow}-\Delta_{\downarrow\uparrow} = 0$. We further separate the case of $(\Delta_x,\Delta_y,0)$ and $(0,0,\Delta_z)$, due to strong anisotropy already present in the model.

Taking the first case, we redefine them in chiral basis with $\Delta_\pm = \frac{1}{\sqrt{2}}(\Delta_x\pm i\Delta_y)$. For further investigation, a GL free energy functional can be derived from microscopics (as done in [6]) for two component order parameter $\Delta_\pm$. This yields the free energy as

$$
F = \sum_{s=\pm}\left\{-|\Delta_s|^2+|D_x\Delta_s|^2+|D_y\Delta_s|^2+\beta_z|D_z\Delta_s|^2+\beta_\perp(D_{-s}\Delta_s)^*D_s\Delta_{-s}+\frac{|\Delta_s|^4}{2}+\frac{\gamma}{2}|\Delta_s|^2|\Delta_{-s}|^2\right\}
$$
$$(3.6)$$

such that the net free energy functional is given as $\mathrm{F} = h_0^3 l_m^3\int\big(F(\vec{R})+\vec{B}\cdot\vec{B}\big)$.

Various scalings have been done, starting with a scaled order parameter, $\vec{R}$ as being a scaled coordinate, scaled vector potential $\vec{a}(\vec{R})$ s.t. $\nabla \times \vec{a} = \vec{B}$ and the operator $D_{\pm} = (D_x \pm iD_y)$ in which $\vec{D} = -(\frac{i}{\kappa})\nabla_{\vec{R}} + \vec{a}(\vec{R})$ with the dimensionless coupling constant κ that characterizes the penetration depth. All these have been explicitly mentioned in Appendix A along with other parameters $\beta_z, \beta_\perp \& \gamma$.

3.4   Uniform Solutions for the GL functional

The above free energy functional is similar to the one derived in the previous chapter, differing by gradient along z directions (which we'll eventually set to be zero for the case of 2D plane). This term arises from the interaction between SOC and two component order parameter.

However, similar to the case for functional in the previous chapter, the value of γ determines the state of the uniform solution: for $\gamma > 1$ implies a time reversal broken chiral phase while $0 < \gamma < 1$ implies a spontaneously rotational symmetry broken state. For the first, the order parameter $\vec{\Delta} = \Delta_0(1, \pm i, 0)$ while for the second $\vec{\Delta}(\vec{r}) = \Delta_0(cos(\theta), sin(\theta), 0)$ for some real constant $|\Delta_0| = 1/\sqrt{1 + \gamma}$.

3.5   Spin Polarization

We now change gears and focus on another related property of the states, namely spin polarization. The nematic state preserves time reversal, hence cannot have a nonzero spin polarization.

However the chiral state breaks time reversal and can feature nonzero value of spin polarization. We now state expression for spin polarization using anomalous green's function technique, which has been calculated in [6]. The final result is stated here for brevity.

The final result is given by

$$\vec{S}(\vec{r}) = \frac{T}{2} \int \frac{d^3\vec{p}}{(2\pi)^3} \frac{v^2 p_\perp^2 + 2v_z^2 p_z^2}{E_+(\vec{p})^2} \frac{i\left[\vec{\Delta}(\vec{r}) \times \vec{\Delta}^*(\vec{r})\right]}{(i\omega_n + \mu - E_+(\vec{p}))^2(i\omega_n - \mu + E_+(\vec{p}))} \tag{3.7}$$

$$+\frac{vT|\Delta|^2}{16} \sum_n \int \frac{d^3\vec{p}}{(2\pi)^3} \frac{v^2 p_\perp^2}{E_+(\vec{p})^2} \frac{Im(\Delta_1^*(\vec{r})[\hat{z} \times \nabla \Delta_1(\vec{r})] - \Delta_2^*(\vec{r})[\hat{z} \times \nabla \Delta_2(\vec{r})])}{[\omega_n^2 + (E_+(\vec{p}) - \mu)^2]^2} \tag{3.8}$$

If we set the intraorbital pairing $\Delta_{1,2} = 0$, we get $S(\vec{r}) \propto \left|\vec{\Delta}(\vec{r}) \times \vec{\Delta}^*(\vec{r})\right|$. For a nematic phase, the OPs are real and hence there's no local spin polarization. However, for the chiral state, due to time reversal breaking, we have local polarization. However, as we'll see in the next chapter, it is indeed possible to have non-zero local spin polarization in the case of half quantum vortex bound pair in the nematic phase.

Chapter 4

Spin Polarization of HQV

Nematic state breaks spontaneous rotational symmetry however still preserves time reversal symmetry. On account of this we expect nematic state to be non-spin polarised. However near the core of these vortex states due to difference in the magnitude of the two order parameters a complete time reversal symmetry is absent. Hence we expect a spin polarisation near the core, which would decrease(and ultimately vanish) in the bulk of the super conductor. Also naïvely we expect that opposite windings of two half quantum vortices would lead to opposite spin polarisation, ultimately cancelling out the net contribution.

To do a quantitative analysis of the same, we take a pair of half quantum vortices separated by a internuclear distance less than penetration depth ($r_{12} < \lambda$). One can redo this analysis for isolated half quantum vortex, however given the instability of a single vortex, we take the more realistic situation of a tightly bounded pair that is likely to be observed in experiments (and has been observed numerically in [6]).

We take the Eqn(2.16) as our form of 2 component order parameter

$$(\eta_+, \eta_-) = \eta_\infty (\ e^{i(\phi_1 + \theta_\infty)} f(r_1), \ f(r_2) e^{i(\phi_2 - \theta_\infty)} \ ) \tag{4.1}$$

where $f(r) = \Theta(\frac{r}{\xi} - 1) + \frac{r}{\xi}\Theta(1 - \frac{r}{\xi})$.

This corresponds to two side by side vortex sttructures with cylindrical symmetry at an intervortex distance $d \ll \xi$ (hence the non-linear structure of the vortex core is taken into account). Plugging this into Eqn(3.8), we have

$$\vec{S}(\vec{r}) = \frac{T}{2} \int \frac{d^3\vec{p}}{(2\pi)^3} \frac{v^2 p_\perp^2 + 2v_z^2 p_z^2}{E_+(\vec{p})^2} \frac{i\left[\vec{\Delta}(\vec{r}) \times \vec{\Delta}^*(\vec{r})\right]}{(i\omega_n + \mu - E_+(\vec{p}))^2(i\omega_n - \mu + E_+(\vec{p}))} \tag{4.2}$$

$$= \frac{-T}{4} \int \frac{d^3\vec{p}}{(2\pi)^3} \frac{v^2 p_\perp^2 + 2v_z^2 p_z^2}{E_+(\vec{p})^2} \frac{|\eta_+|^2 - |\eta_-|^2}{(i\omega_n + \mu - E_+(\vec{p}))^2(i\omega_n - \mu + E_+(\vec{p}))}\hat{z} \tag{4.3}$$

Now we can analyze the solution casewise:-

- In case the vortices don't overlap with one another, $\vec{S}(\vec{r})$ is localized to the individual vortex cores and beyond $r = \xi$ distance of each core, it simply vanishes. Now the distribution of $S(r)$ vs r is an increasing function and goes quadratically with r i.e. $\propto r^2$. This however is due to the linear increase ansatz taken for the core $f(r) \sim \frac{r}{\xi}$. However, a more accurate (and smoother) choice should be $f(r) \sim tanh(\frac{\nu r}{\xi})$, where $\nu \sim 1$ (as is the case for usual vortices). Thus we see that with increasing r, the spin polarization increases (decreases) from the vortex and then settles to 0 ultimately. This makes the net spin polarization 0 for the whole system.

- In case the vortices overlap significantly (i.e $d \ll \xi$), let O_i be the region of each core. Then similar to the case above the spin polarization vanishes in the region $O_1^C \cap O_2^C$. In the region of $O_1/(O_1 \cap O_2)$, we have $S(r) \propto r^2$ as the case above and similarly for $O_2/(O_1 \cap O_2)$ (with $S(r) \propto -(\vec{r} - d\,\hat{i})^2$) (assuming + sign for the vortex at origin, and the second vortex being placed at (d,0,0)). However for the region $O_1 \cap O_2$, we have $S(r) \propto r^2 - (\vec{r} - d\,\hat{i})^2$. This is essentially overlapping the two initial $S(r)$ distributions present around initially isolated points.

We plot the Spin polarization $\vec{S}(\vec{r})$ for different vortex configurations as follows:-
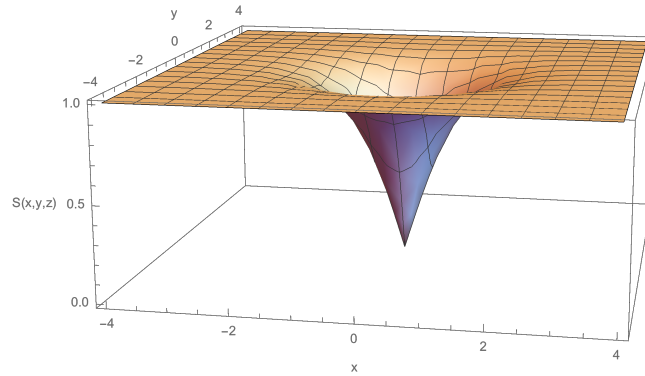
- For the case of a single half quantum vortex

Figure 4.1: Plot of Spin polarization for a single HQV

We see that the Spin polarization peaks at the vortex center and decays with the characteristic length ξ as we move away from the vortex. However, as discussed before, this configuration is unstable, as it has divergent energy cost scaling with system size. For the purposes of plotting, the characteristic profile of $\psi \sim tan(x/\xi)$ is taken.

- For a pair of HQV, which is a stable configuration, we again plot the profile. This is done by taking the vortex core ψ similar to usual s-wave vortices
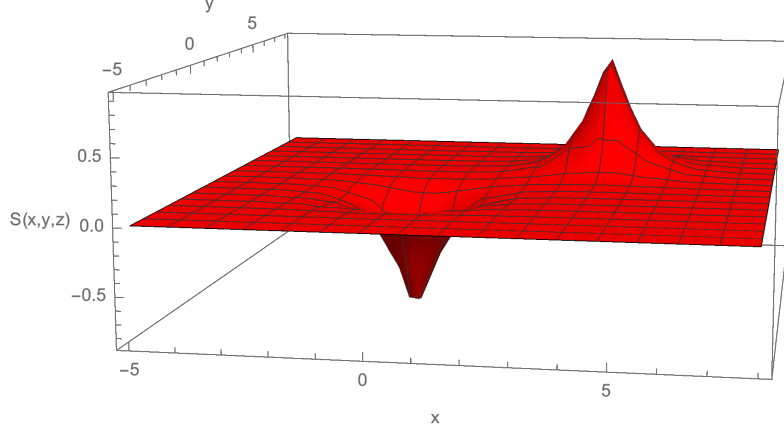
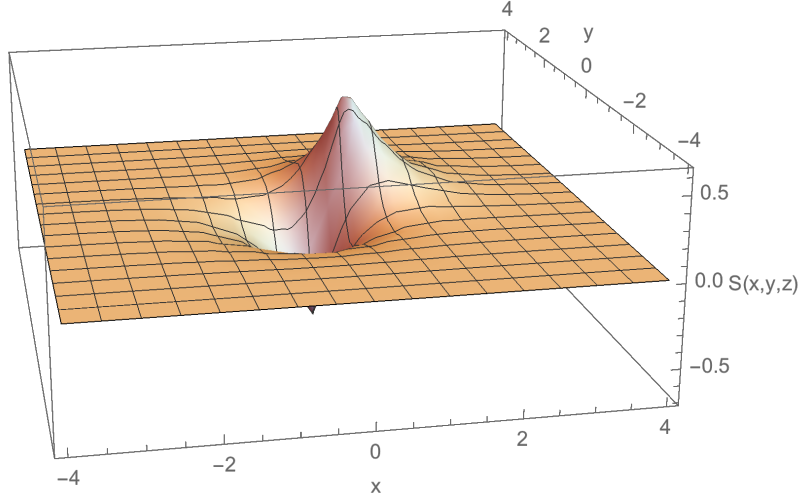**Figure 4.2:** Plot of Spin polarization for HQV pair separated away

Figure 4.3: Plot of Spin polarization for HQV pair while overlapping

We see that the net Spin polarization is opposite for two oppositely wounded vortices, while locally $S(\vec{r}) \neq 0$. As the vortices start overlapping, the local contributions add and cancel each other.

Thus we see that indeed the net spin polarization is 0 with a nonzero local profile. This can serve as an important identifier for the HQV state, as it carries a spin current absent in conventional vortices. The corresponding phenomena in superfluid He_A^3 phase and p-wave pairing Sr_2RuO_4 was studied in [4], reaching the conclusion of an additional (i.e. in addition to zeeman coupling) spin polarization at equilibrium. There it was indicated that the order of contributions due to spin polarization by zeeman and spin vortex (which corresponds to nematic vortex in this thesis) being equal, opens the possibility of experimental determination of half quantum vortices. Moreover, in the same reference [4], the authors commented that a spin current near a HQV can generate effective electric field which can then be measured. This is something that could be investigated within the context of the above analysis too. Also, as pointed in [3],local density of states probed by

STM may show a twin-peak structure due to the HQV pair. This makes this particular study important in the current search for explanations regarding superconductivity in $M_X Bi_2 Se_3$.

Chapter 5

Conclusion

In this report we've managed to discuss Half quantum vortices in odd parity supercon-
ductors and presence of half quantum vortices in them. As we saw in, presence of multiple
order parameters opens up the possibility of fractional flux quanta and fractional vortex
dynamics. However, energetic still dictate as to whether or not a given HQV pair will be
observed, albeit numerically they've been reported as stable solutions. We also see that
presence of HQV pair is also characterised by non-zero spin polarisation and this, along
with other features, can be used to study the existence of HQV bound pair. Moreover,
as remarked in [3], this also serves as way to reject/ accept the nematic hypothesis.

Bibliography

[1]   Zhitomirskii M. E. "Magnetic transitions in a superconducting UPt3". In: *Phys. Rev. Lett.* 103 (5 July 2009), p. 057003. DOI: 10.1103/PhysRevLett.103.057003. URL: https://link.aps.org/doi/10.1103/PhysRevLett.103.057003.

[2]   Liang Fu and Erez Berg. "Odd-Parity Topological Superconductors: Theory and Application to $Cu_xBi_2Se_3$". In: *Phys. Rev. Lett.* 105 (9 Aug. 2010), p. 097001. DOI: 10.1103/PhysRevLett.105.097001. URL: https://link.aps.org/doi/10.1103/PhysRevLett.105.097001.

[3]   Pye Ton How and Sung-Kit Yip. "Half quantum vortices in a nematic superconductor". In: *Phys. Rev. Research* 2 (4 Nov. 2020), p. 043192. DOI: 10.1103/PhysRevResearch.2.043192. URL: https://link.aps.org/doi/10.1103/PhysRevResearch.2.043192.

[4]   Victor Vakaryuk and Anthony J. Leggett. "Spin Polarization of Half-Quantum Vortex in Systems with Equal Spin Pairing". In: *Phys. Rev. Lett.* 103 (5 July 2009), p. 057003. DOI: 10.1103/PhysRevLett.103.057003. URL: https://link.aps.org/doi/10.1103/PhysRevLett.103.057003.

[5]   Jörn W. F. Venderbos, Vladyslav Kozii, and Liang Fu. "Identification of nematic superconductivity from the upper critical field". In: *Phys. Rev. B* 94 (9 Sept. 2016), p. 094522. DOI: 10.1103/PhysRevB.94.094522. URL: https://link.aps.org/doi/10.1103/PhysRevB.94.094522.

[6]   A. A. Zyuzin, Julien Garaud, and Egor Babaev. "Nematic Skyrmions in Odd-Parity Superconductors". In: *Phys. Rev. Lett.* 119 (16 Oct. 2017), p. 167001. DOI: 10.1103/PhysRevLett.119.167001. URL: https://link.aps.org/doi/10.1103/PhysRevLett.119.167001.